Available online at www.sciencedirect.com

ScienceDirect

Current Opinion in Structural Biology

Multicolor single-molecule FRET studies on dynamic protein systems

Ecenaz Bilgen and Don C. Lamb

Förster resonance energy transfer (FRET) is a powerful tool for studying protein conformations, interactions, and dynamics at the single-molecule level. Multicolor FRET extends conventional two-color FRET by incorporating three or more fluorophores and thereby enabling a more comprehensive view of complex biomolecular processes. This technique allows for the simultaneous tracking of multiple structural changes, detecting intermediate states, and resolving heterogeneous population distributions. In this review, we discuss the recent advancements in fluorophore labeling strategies and data analysis methods that have significantly improved the precision and applicability of multicolor FRET in protein studies. We then end this review by showcasing recent applications for investigating protein folding and processes involved in gene regulation.

Addresses
Department of Chemistry and Center for Nanoscience, Ludwig-Maximilians-Universität Munich, 81377, Munich, Germany

Corresponding author: Lamb, Don C. (don.lamb@cup.uni-muenchen.de)

Current Opinion in Structural Biology 2025, **93**:103117

This review comes from a themed issue on **Biophysical Methods (2025)**

Edited by **Hoi Sung Chung** and **Francesca Marassi**

For complete overview of the section, please refer the article collection - Biophysical Methods (2025)

Available online 14 July 2025

https://doi.org/10.1016/j.sbi.2025.103117

Introduction

Measurements of Förster resonance energy transfer (FRET) at the single molecule level have been recognized as a universal tool for studying the conformation and dynamics of macromolecules [1–3]. Briefly, when spectrally overlapping fluorescent molecules are in close proximity, the excited donor (D) molecule can transfer its energy to an acceptor (A) molecule with an efficiency that depends on the inverse sixth power of the donor–acceptor separation [4]. Thus, FRET is very sensitive to distance changes within the range of 2–12 nm (or 20–120 Å). Single-molecule FRET (smFRET) has changed the way we see the biological world due to its power to resolve individual conformational states in heterogeneous mixtures and the dynamics within them. Compared to other biophysical techniques, smFRET experiments have the advantage of being able to study molecules under physiological conditions and require sub-attomoles of the labeled sample. Traditionally, smFRET measurements depend on one D-A pair to probe a single distance at a time. However, it is now possible to probe coordinated motions in multiple dimensions by fluorescence labeling of three [5] or four [6] distinct positions. This provides more information for hybrid structural biology, making it possible to investigate allosteric effects in proteins or investigate structural changes in the presence or absence of other biomolecules (Figure 1a).

Three and four-color FRET experiments were first designed to investigate dynamics of nucleic acid systems such as holiday junctions [5,6] and DNA origami structures [7,8] as well as DNA-protein assemblies [9]. However, up until recently, most multicolor FRET studies have been proof-of-principle experiments yielding some exciting results, but the number of challenges involved in such experiments have kept the method from being widely utilized. With the advancement in labeling chemistries, fluorescent dyes, and data collection and analyses approaches, multicolor FRET is now more broadly applicable and can be used to investigate more complex bimolecular machineries. This review begins with a brief description of three-color FRET followed by an overview of recent efforts to overcome the challenges of multicolor FRET experiments. The last part of this review summarizes the latest multicolor FRET applications in biomolecular systems.

Three-color FRET

An example of the energy transfer phenomenon between the three fluorophores is shown in Figure 1b. Here, the donor molecule is in close proximity to two acceptors (A_1 and A_2), the first of which can also act as a donor to A_2 (hence referred to as $A_1(D_2)$). Energy transfer can take place between all three FRET pairs D_1-$A_1(D_2)$, D_1-A_2, and $A_1(D_2)$-A_2, which allows the simultaneous observation of distance changes between all three FRET pairs, but complicates the analysis [9,10]. A qualitative assessment of FRET efficiencies between D-A_1 and D-A_2 can be derived from the raw signal fractions in the donor and acceptor channels

Figure 1

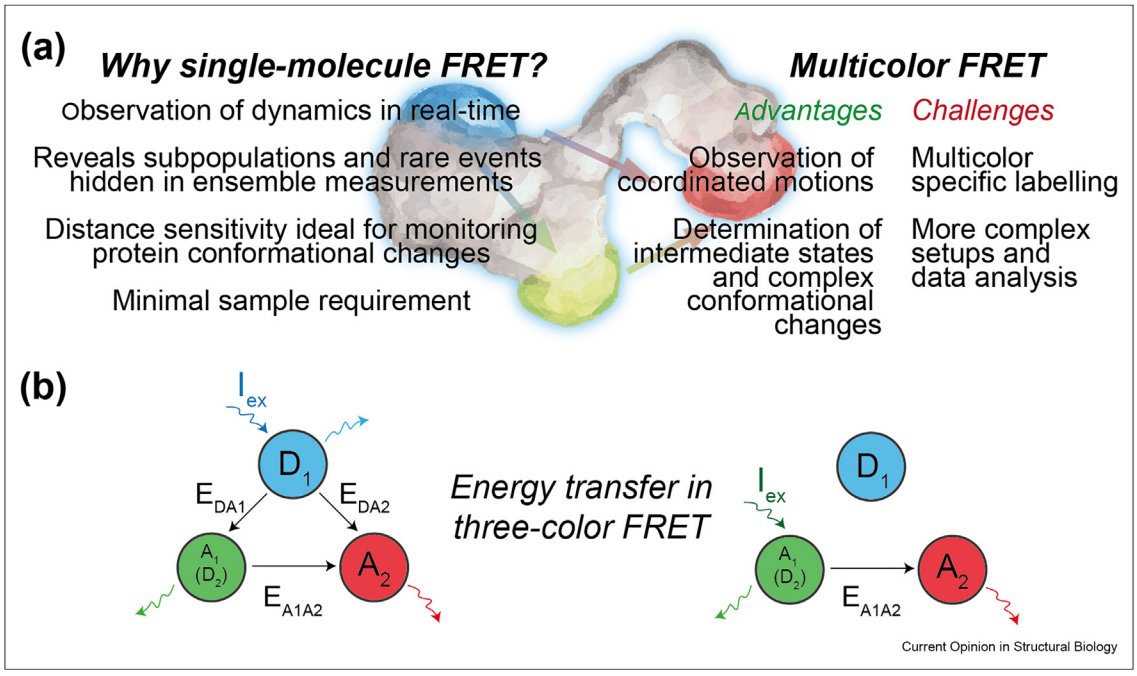

An overview of single-molecule FRET and multicolor FRET applications on proteins. (a) An artistic representation of a protein containing three fluorophores along with a list of benefits and challenges for such measurements**. b)** Diagram of energy transfer pathways in a three-color FRET system after donor dye (D_1) excitation (blue, *left*) or acceptor 1/donor 2 ($A_1(D_2)$) excitation (green, *right*). Energy can be transferred to either acceptor $A_1(D_2)$ or A_2 (green and red, respectively) with transition probabilities E_{DA1} and E_{DA2}. Additionally, $A_1(D_2)$ can transfer energy to A_2 with a FRET efficiency of $E_{A1(D2)\ A2}$. Energy transfer can also take place after direct excitation of acceptor $A_1(D_2)$.

following donor excitation ($I_{D_1}^{D_{ex}}, I_{A_1/D_2}^{D_{ex}}, I_{A_2}^{D_{ex}}$), referred to as the proximity ratios ($PR_{D_1A_1}$ and $PR_{D_1A_2}$).

$$PR_{DA_1} = \frac{I_{A_1(D_2)}^{D_{ex}}}{I_{D_1}^{D_{ex}} + I_{A_1(D_2)}^{D_{ex}} + I_{A_2}^{D_{ex}}}; PR_{DA_2} = \frac{I_{A_2}^{D_{ex}}}{I_{D_1}^{D_{ex}} + I_{A_1(D_2)}^{D_{ex}} + I_{A_2}^{D_{ex}}} \quad (1)$$

However, unlike two-color FRET, these values do not directly correspond to distances. In three-color FRET systems, energy transfer can, in general, occur between all three dye pairs, meaning that the efficiency of transfer to one acceptor is influenced by the quenching effect of the second acceptor. The apparent FRET efficiencies from the donor dye to each acceptor, ($E'_{D_1A_1}$ *and* $E'_{D_1A_2}$), represent the transition probabilities within the three-color FRET system and are related to the single-pair FRET efficiencies ($E_{D_1A_1(D_2)}$ and $E_{D_1A_2}$) by:

$$E_{DA_1(D_2)} = \frac{I_{A_1(D_2)}^{D_{ex}}}{I_D^{D_{ex}}\left(1 - E_{A_1(D_2)A_2}\right) + I_{A_1(D_2)}^{D_{ex}}} \quad (2)$$

$$E_{DA_2} = \frac{I_{A_2}^{D_{ex}} - E_{A_1(D_2)A_2}\left(I_{A_1(D_2)}^{D_{ex}} + I_{A_2}^{D_{ex}}\right)}{I_D^{D_{ex}} + I_{A_2}^{D_{ex}} - E_{A_1(D_2)A_2}\left(I_D^{D_{ex}} + I_{A_1(D_2)}^{D_{ex}} + I_{A_2}^{D_{ex}}\right)} \quad (3)$$

Thereby, one compensates for the competition between the two acceptors for energy transfer from the donor as well as energy transferred between $A_1(D_2)$ and A_2, and hence, retrieves the FRET efficiency between the three dye pairs as if each dye pair was isolated. Of course, as for two-color experiments, additional corrections are necessary to obtain the corrected or absolute FRET efficiencies. For three-color FRET, all three dyes are typically selected from the visible region of the spectrum and have limited spectral separation. This leads to spectral crosstalk (*ct*), which can be significantly higher than in the two-color FRET case, as well as direct excitation (*de*) of the two acceptor fluorophores. In addition, the quantum yield of the fluorophores and the detection efficiency over the visible region can change significantly, leading to different detection efficiencies (γ) in the three channels. When taking into account the various correction factors, the FRET efficiencies are given by:

$$E_{A_1(D_2)\,A_2} = \frac{I_{A_2}^{A_1(D_2)_{\mathrm{ex}}} - ct_{A_1(D_2)\,A_2} I_{A_1(D_2)}^{A_1(D_2)_{\mathrm{ex}}} - de_{A_2}^{A_1(D_2)_{ex}} I_{A_2}^{A_{2\mathrm{ex}}}}{\gamma_{A_1(D_2)\,A_2} I_{A_1(D_2)}^{A_1(D_2)_{\mathrm{ex}}} + I_{A_2}^{A_1(D_2)_{\mathrm{ex}}} - ct_{A_1(D_2)\,A_2} I_{A_1(D_2)}^{A_1(D_2)_{\mathrm{ex}}} - de_{A_2}^{A_1(D_2)_{ex}} I_{A_2}^{A_{2\mathrm{ex}}}} \tag{4}$$

$$E_{DA_1(D_2)} = \frac{I_{A_1(D_2)}^{D_{\mathrm{ex}},\mathrm{cor}}}{\gamma_{DA_1(D_2)} I_D^{D_{\mathrm{ex}}} \left(1 - E_{A_1(D_2)\,A_2}\right) + I_{A_1(D_2)}^{D_{\mathrm{ex}},\mathrm{cor}}} \tag{5}$$

$$E_{DA_2} = \frac{I_{A_2}^{D_{\mathrm{ex}},\mathrm{cor}} - E_{A_1(D_2)\,A_2}\left(\gamma_{A_1(D_2)\,A_2} I_{A_1(D_2)}^{D_{\mathrm{ex}},\mathrm{cor}} + I_{A_2}^{D_{\mathrm{ex}},\mathrm{cor}}\right)}{\gamma_{D\,A_2} I_D^{D_{\mathrm{ex}}} + I_{A_2}^{D_{\mathrm{ex}},\mathrm{cor}} - E_{A_1(D_2)\,A_2}\left(\gamma_{D\,A_2} I_D^{D_{\mathrm{ex}}} + \gamma_{A_1(D_2)\,A_2} I_{A_1(D_2)}^{D_{\mathrm{ex}},\mathrm{cor}} + I_{A_2}^{D_{\mathrm{ex}},\mathrm{cor}}\right)} \tag{6}$$

where

$$I_{A_1(D_2)}^{D_{\mathrm{ex}},\mathrm{cor}} = I_{A_1(D_2)}^{D_{\mathrm{ex}}} - ct_{DA_1(D_2)} I_D^{D_{\mathrm{ex}}} - de_{A_1(D_2)}^{D_{ex}} I_{A_1(D_2)}^{A_1(D_2)_{\mathrm{ex}}} \tag{7}$$

$$I_{A_2}^{D_{\mathrm{ex}},\mathrm{cor}} = I_{A_2}^{D_{\mathrm{ex}}} - de_{A_2}^{D_{ex}} I_{A_2}^{A_{2\mathrm{ex}}} - ct_{D\,A_2} I_D^{D_{\mathrm{ex}}} - ct_{A_1(D_2)\,A_2}\left(I_{A_1(D_2)}^{D_{\mathrm{ex}}} - ct_{D\,A_1(D_2)} I_D^{D_{\mathrm{ex}}}\right) - de_{A_1(D_2)}^{D_{ex}} E_{A_1(D_2)\,A_2}\left(1 - E_{A_1(D_2)\,A_2}\right)^{-1} I_{A_1(D_2)}^{A_1(D_2)_{\mathrm{ex}}} \tag{8}$$

Current advances in multicolor FRET studies

Multicolor FRET measurements in solution

Solution-based smFRET experiments are based on measuring freely diffusing molecules at picomolar concentration on a confocal microscope. The fluorescently labeled biomolecules generate single-molecule bursts as they diffuse through the detection volume. For multicolor FRET experiments, the setup needs to be equipped with either alternating laser excitation (ALEX) [11,12] or pulsed interleaved excitation (PIE) [13] as it is necessary to directly excite $A_1(D_2)$ to calculate all three FRET efficiencies. A schematic of our confocal setup equipped with multiparameter fluorescence detection (MFD) and pulsed interleaved excitation (PIE) for three-color smFRET is shown in Figure 2a. The use of nanosecond ALEX/PIE allows determination of the fluorescence lifetime of the captured bursts, which is useful to assess conformational dynamics taking place faster than the diffusion time. Using fluorescence correlation spectroscopy [14] or the dynamic photon distribution analysis [15], the dynamics can be quantified on the ~100 ns to ms timescale. Employing ALEX or PIE in multicolor FRET experiments also offers the possibility to directly determine the correction factors required for reporting accurate FRET efficiencies [16]. However, extracting precise distance information from three-color FRET experiments remains difficult. The main challenge is the high amount of noise in such experiments. First, the fluorescence intensity after donor excitation is divided across three detection channels. Secondly, as the best fluorophores are in the blue to red region of the visible spectrum, the close spectral proximity of three fluorophores in this region leads to

Figure 2

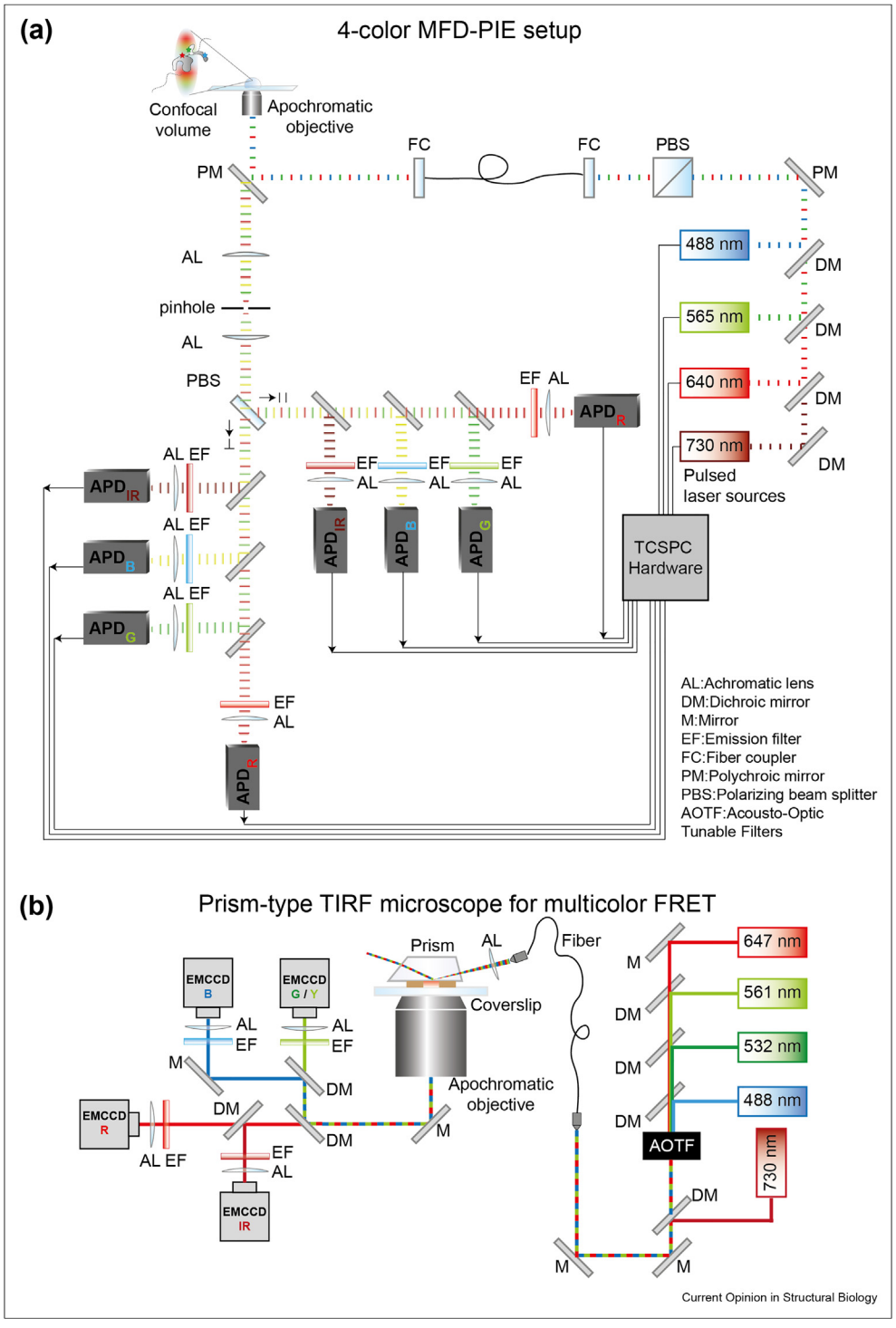

Experimental setups for measuring multicolor FRET. a) Scheme of a four-color MFD-PIE confocal setup. **b)** Scheme of a prism-type TIRF microscope for multicolor FRET experimentation. AL:Achromatic lens, M:Mirror, DM:Dichroic mirror, EF:Emission filter, FC:Fiber coupler, PM:Polychroic mirror, BS:Polarizing beam splitter, AOTF:Acousto-Optic Tunable Filters.

significant spectral crosstalk and direct excitation. With the number of corrections required to quantify the distance between the three fluorophores, the analysis becomes demanding.

In order to overcome these challenges, we introduced a three-color photon distribution analysis (3C-PDA) [17], which expands on PDA introduced by the group of Claus Seidel [18] and introduces a likelihood function describing the three-color FRET process in diffusion-based experiments. With this statistical approach, we incorporated all necessary experimental correction factors into the analysis and then compared the resulting proximity ratios to those of the background corrected data, avoiding additional noise upon correcting the FRET data. 3C-PDA can be used to simultaneously describe three distances in the conformational space of a biomolecule and reveal coordinated conformational transitions. All of the above-mentioned burst analysis tools are implemented in our open-source software package PIE analysis with MATLAB (PAM) [19].

Multicolor FRET on surface-immobilized molecules

Depending on the system of interest, smFRET experiments can be done on surface-immobilized molecules using total internal reflection fluorescence (TIRF) microscopy [20]. A schematic of our prism-type multicolor TIRF microscope setup with millisecond alternating laser excitation (msALEX) [11,12] is shown in Figure 2b. msALEX is typically performed using an Acousto-Optic Tunable Filter (AOTF) but modern lasers also allow direct modulation of the signal. The excitation beam travels through a quartz prism and utilizes the interface between the quartz and the aqueous solution to generate total internal reflection. The sample molecules are immobilized on the prism surface so that they can be illuminated by the evanescent field. Conformational changes happening from seconds to minutes can be captured directly in smFRET experiments. When expanding the color palette of these experiments to three colors and beyond, the challenges of quantitative data analysis on single-molecule trace statistics become more pronounced. For instance, the measured datasets are larger in multicolor FRET experiments since a lower fraction of molecules contain all three fluorophores, a large portion of the traces suffer from low signal-to-noise ratios and/or dye photophysics. Manual data sorting becomes more intense due to both the increasing number of channels in multicolor FRET experiments and the larger data sets. It has been shown that deep learning can be used for rapid and automated analysis of smFRET traces [21–23]. However, these applications were limited to the classification of dual-color FRET data. Recently, we expanded the previous work on automated trace classification software and developed the open-source Deep-Learning Assisted, Single-molecule Imaging (Deep-LASI) package for analysis of FRET data up to three colors [24,25]. Deep-LASI offers visualization of corrected and apparent FRET efficiencies, transition density plots between different FRET states, and extraction of the kinetic rates between them.

Protein labeling for multicolor FRET studies

The next major challenge for multicolor FRET is specifically labeling biomolecules with three or more fluorophores. While this can be done with nucleotides or for protein-nucleic acid complexes, the specific, fluorescent labeling of proteins at more than two positions is not straightforward. The conventional stochastic labeling approach used for dual-color FRET labeling is not applicable to three-color experiments as it would result in a combination of six different labeling configurations. One can reduce the complexity to two configurations by combining stochastic labeling with different labeling techniques for the third fluorophore, such as incorporation of non-canonical amino acids (ncAA) [26]. Three-color specific labeling can be performed by expressing and labeling two parts of the protein independently and then using sortase-mediated ligation to combine them and thereby generating a cysteine residue for specific labeling with a third fluorophore [27,28]. Recently, we presented a three-color labeling protocol for a double mutant of the maltose-binding protein (MBP) [29]. The first position was labeling with Atto488 using a ncAA and copper-catalyzed azide–alkyne cycloaddition (CuAAC). We then took advantage of maltose binding to block accessibility to a cysteine residue on the surface of the maltose binding pocket following the approach of Jager et al. [30]. In the presence of saturating maltose concentrations, only one surface accessible cysteine was available and Alexa647 could be selectively attached to the second labeling position. After the removal of maltose, the second cysteine could be labeled with Atto565, yielding a specific three-color labeled MBP.

In a recent work by Bonhomme et al., the dimeric human metabotropic glutamate receptor 2 (mGlu2) could be successfully labeled at three positions with three distinct labeling chemistries (Figure 3) [31]. They genetically encoded two ncAA utilizing two different stop codons in combination with fusion to a genetically encoded self-labeling SNAP-tag (Figure 3a). In the first protomer, a SNAP-tag is fused to the N-terminal along with a p-propargyloxy-L-phenylalanine (PrF) in response to the Amber codon (TAG) (Figure 3a). In the second protomer, no SNAP tag was used and a trans-cyclooct-2-en-L-lysine (TCOK) was incorporated in response to an

Figure 3

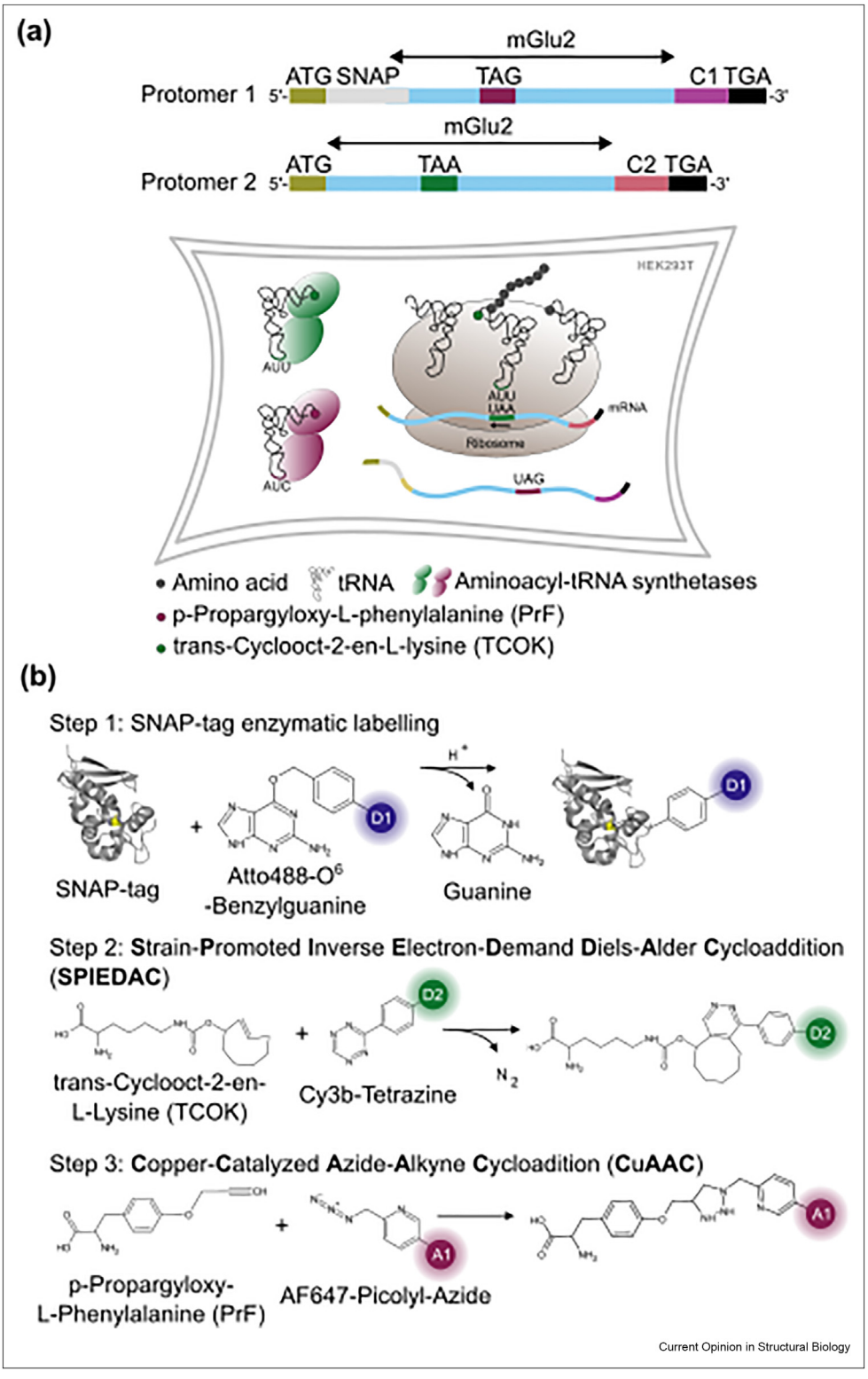

Site-specific three-color labeling of the metabotropic glutamate receptor 2. a) Schematic representation of the mGlu2 protomer genes expressed to produce a specifically-labeled 3-color smFRET sensor. **b)** The three orthogonal site-specific labeling reactions used for labeling the mGlu2 receptors in the membrane of living cells: 1) SNAP-tag labeling using Atto488-06-benzylguanine; 2) TCOK labeling using Cy3B-Tetrazine; and 3) PrF labeling using AF647-Picolyl-Azide. Adapted from Ref. [31].

Figure 4

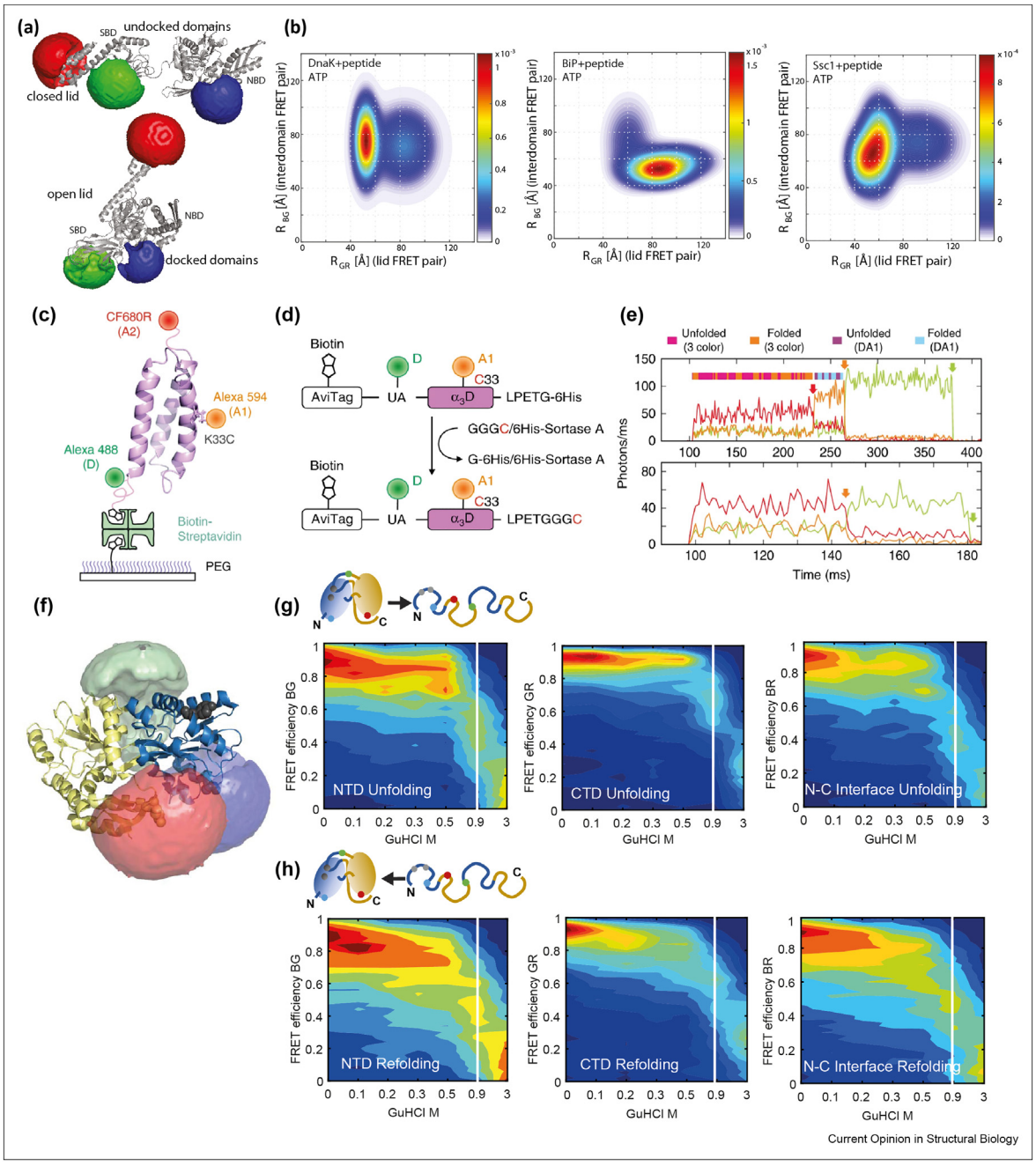

Multicolor single-molecule FRET studies on proteins. a) Accessible volume calculations for the fluorophores Atto488, Atto565, and Atto647N attached to the Hsp70 homolog DnaK in the ADP- (PDB:2KHO, top) and ATP-bound (PDB:4B9Q, bottom) states, respectively. **b)** From left to right: Two-dimensional apparent distance distributions of the interdomain distance (R_{BG}) versus the lid conformation (R_{GR}) in the presence of a model substrate and ATP for DnaK, BiP and Ssc1, respectively. Adapted from Ref. [26]. **c)** Surface immobilized 3-color FRET construct for the α_3D protein showing the labeling positions of the three fluorophores. **d)** Site specific labelling scheme for the α3D peptide. Alexa 488 is conjugated to 4-acetylphenylalanine (UA) at the N-terminus, Alexa 594 (acceptor 1, A1) is linked to a cysteine at residue 33. An additional cysteine residue is introduced at the C-terminus via sortase-mediated ligation of a short GGGC peptide and subsequently labeled with CF680R (acceptor 2, A2). **e)** Two α_3D fluorescence trajectories of the donor (green), acceptor 1 (orange), and acceptor 2 (red) at 2.25 M GdmCl. In the upper trajectory, folding/unfolding is monitored with all three fluorophores until A2 photobleaches (indicated by the red arrow) followed by A1 photobleaching (orange arrow). The states identified by the Viterbi algorithm are represented in the color bar above the upper trajectory. In the lower trajectory, dynamics are followed until A2 photobleaches at around 145 ms (orange arrow). Adapted from Ref. [41]. **f)** Structure of MBP (PDB ID:1OMP; NTD in yellow, CTD in blue) showing the accessible volumes available for Atto488 (blue), Atto565 (green) and Alexa647 (red) at the labeling positions A52, K175 and P298, respectively. **g-h)** Waterfall plots of the FRET efficiency versus GuHCl concentration following the conformational changes in the NTD (BG, left), CTD (GR, middle) and at the N−C interface (BR, right) during equilibrium unfolding (G) and refolding (H). The white line separates the 0.9 M GuHCl measurement from the higher denaturant concentrations. Adapted from Ref. [29].

Figure 5

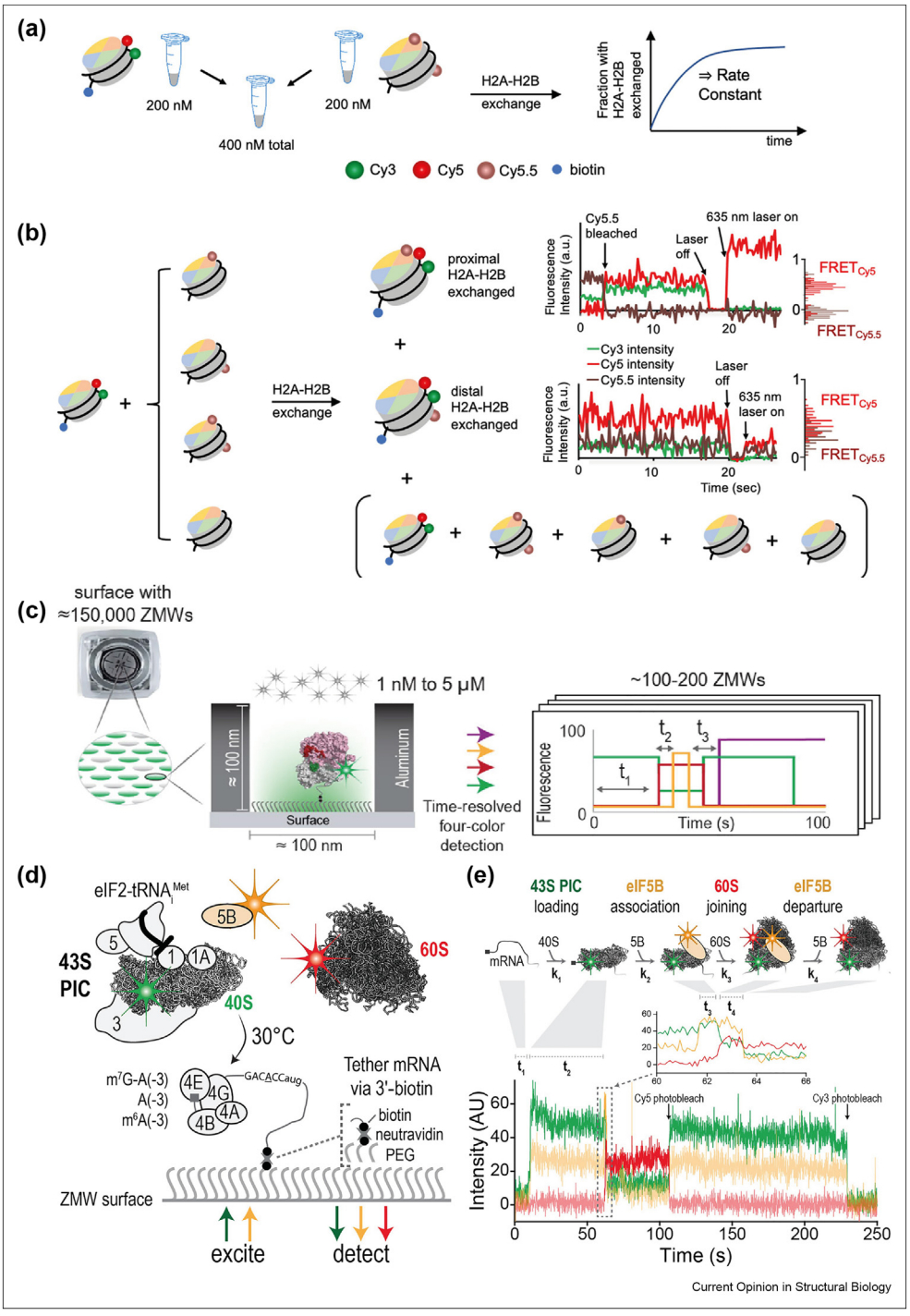

Experimental approach for tracking the kinetics of histone H2A-H2B exchange between nucleosomes. **a)** Equimolar concentrations of two distinct nucleosome types, each labeled differently, are combined to a total concentration of 400 nM under various conditions to observe the kinetics of nucleosomes undergoing H2A-H2B exchange. **b)** The possible pathways leading to detectable H2A-H2B exchange using the three-color smFRET setup are illustrated. The mixing of the labeled batches shown in (A) produces proximal or distal H2A-H2B histone exchange. Two example traces showing proximal (upper trace) and distal (lower trace) exchange along with histograms of the $FRET_{Cy5}$ (red) and $FRET_{Cy5.5}$ (brown) efficiencies shown to the side of the traces (even after photobleaching of Cy5.5). In the case of proximal H2A-H2B exchange, high $FRET_{Cy5.5}$ and low $FRET_{Cy5}$ signals are detected, which leads to fast photobleaching of Cy5.5. In the case of distal H2A-H2B exchange, low-mid $FRET_{Cy5}$, and non-zero $FRET_{Cy5.5}$ signals are observed. Hence, the distal exchange was analyzed due to the longer FRET traces. The other nucleosomes shown below in the parentheses do not generate any Cy5.5 signals. Adapted from Ref. [52]. **Real time monitoring of the ribosomal subunit formation. c)** A real-time single-molecule fluorescence assay is depicted using zero-mode waveguides (ZMWs). mRNA is tethered to the surface within the individual ZMWs where the reactions are imaged.

Ochre codon (TAA) (Figure 3a). Afterwards, a three-step labeling procedure was performed directly in living mammalian cells using 1) SNAP-tag labeling with Atto488- O^6-benzylguanine, 2) strain-promoted inverse electron-demand Diels–Alder cycloaddition reaction on TCOK with Cy3B-Tetrazine, and a 3) CuAAC reaction on PrF AF647-Picolyl-Azide (Figure 3b). Measurements of 3-color FRET in combination with 3C-PDA on the labeled construct revealed an intermediate conformational state of mGlu2, which could not be observed by previous 2-color FRET studies. This new triple-labeling strategy is generalizable and can be applied to other protein systems.

Multicolor FRET studies on protein-folding mechanisms

Chaperone proteins

Heat-shock proteins (Hsps) are a class of molecular chaperones that maintain protein homeostasis and are present in single-cell organisms to humans. A widely studied chaperone is the dimeric 90-kDa heat-shock protein (Hsp90) that shows distinct opening-closing motions upon ATP hydrolysis. The movements of the Hsp90 dimer have been observed by dual-color smFRET experiments [32,33]. Hugel and co-workers tackled the Hsp90 chaperone with three- [34] and four-color [35] smFRET experiments and described their multicolor FRET approaches in detail for their potential application to other protein systems [36]. The findings hinted at a more complex conformational landscape where the dimer not only performs opening-closing motions but also undergoes rotational and translational movements. They reported that the dimer opening and closing takes place in milliseconds to minutes, while further local transitions can happen as fast as picoseconds. Hugel et al. recently aimed to bridge the gap between minute-to-picosecond timescale movements in the conformational landscape of Hsp90 by investigating dynamics in the nanosecond regime [37], but in this case using two-color FRET experiments.

Several variants of the 70 kDa heat shock protein (Hsp70) family have been studied in detail including the bacterial Hsp70, DnaK, human BiP from the endoplasmic reticulum and Ssc1 from the mitochondrial matrix of yeast. These homologs show significant structural similarity and are constructed of two domains, the substrate and nucleotide binding domains (SBD and NBD). Upon interaction with ATP, the NBD and SBD are in a docked conformation and the lid of the SBD (SBD-lid) is open. After ATP hydrolysis, the SBD and NBD undock and the SBD-lid closes. The allosteric communication between the SBD and NBD of Hsp70s has previously been studied with dual-color smFRET experiments [16,38,39]. We have recently studied the three Hsp70 homologs, DnaK, BiP and Ssc1, with three-color smFRET where the SBD and NBD docking-undocking and SBD-lid motions could be observed simultaneously for the first time (Figure 4a) [26]. As a labeling strategy, we attached Atto488 (B) site-specifically using a ncAA to the NBD and Atto565 (G) and Atto647N (R) stochastically to the SBD and lid. As the FRET efficiency histograms were similar for the NBD-lid and NBD-SBD dye pairs in two-color experiments, we focused on the FRET efficiency changes between the BG and GR dye pairs. The GR FRET pair reports on the conformation of the lid, independent of the labeling position, whereas the BG FRET pair reports on the domain motion, with a potential additional contribution from the lid depending on the labeling position of the dyes. For large-scale changes between the SBD and NBD, the potential contribution of the lid conformation, depending on the labeling, could be ignored or incorporated into the analysis. Using 3C-PDA, we assessed the correlated, pair-wise changes in the distance distributions (R_{BG}, interdomain FRET pair, and R_{GR}, lid FRET pair (Figure 4b)). These results pointed out that, in the presence of ATP and a model substrate peptide, BiP prefers a more open-lid conformation coupled with a closer interdomain distance than the other homologs. In addition, the width of the FRET distributions suggests that Ssc1 has a more mobile SBD-lid and BiP has more restricted inter-domain motions when compared to DnaK. The unique conformational behavior of each Hsp70 homolog can be linked to the specialized tasks they need to perform according to their cellular residency.

Monitoring protein folding in real time

Protein folding is a challenging process where newly synthesized amino acid chains seek their native 3-dimensional structure in conformational space. Here, multicolor FRET offers direct observation of the different conformations that the protein adopts as it

Time-resolved, four-color fluorescence is recorded across ~150,000 ZMWs after 532 nm laser excitation. Fluorescence signal order and timing are analyzed in ~100–200 ZMWs and association/dissociation kinetics are determined using probability-based models. The cumulative distribution functions were then fit using exponential functions. Adapted from Ref. [54]. **d)** Schematic of the single-molecule three-color FRET experiment performed by Guca et al. The 43S PIC (10 nM, labelled via 40S–Cy3 subunits (green) and eIFs 1, 1A, 3, 5 and eIF2–GTP–Met-tRNAiMet), 20 nM eIF5B–Cy3.5 (orange) and 100 nM 60S–Cy5 (red) subunits were added to the mRNA sequences (m^6A(-3), A(-3), or control m^7G-A(-3)) tethered within ZMWs in the presence of saturating concentrations of eIFs 4A, 4B, 4G and 4E at 30 °C. **e)** Example single-molecule fluorescence traces that depict sequential association of the 43S PIC subunit (green), eIF5B (orange) and the 60S subunit (red). Dwell times corresponding to 43S PIC association (t_1), eIF5B association (t_2), 60S subunit joining (t_3) and eIF5B departure times from the 80S complex (t_4) are marked. In this trace, the loss of the 60S–Cy5 fluorescence signal is attributed to photobleaching of the dye rather than departure of the ribosomal subunit. Adapted from Ref. [55].

searches for the thermodynamically most stable configuration [40]. Chung and co-workers explored protein folding with three-color smFRET and used the fluorescence lifetime information to measure the timescale of the conformational changes during the folding of the designed protein α_3D [27]. In a more recent work, they demonstrated a three-color FRET approach utilizing continuous wave (CW) excitation and analyzed the collected trajectories using a maximum likelihood method (Figure 4c–d) [41]. The designed construct was site-specifically labeled where Alexa488 was attached to a 4-acetylphenylalanine (UA) residue at the N-terminus and Alexa594 was labeled to a cysteine residue at position 33. The third fluorophore, CF608R, was introduced at the C-terminus to a cysteine that was introduced by sortase-mediated ligation of a short peptide sequence (GGGC, Figure 4c). Their proof-of-concept measurements on folding of the previously described α_3D protein showed that their method can resolve fast kinetics and reduce background signals and photophysical artefacts.

The folding process is more complex for large, multi-domain proteins, which often require assistance from chaperones to achieve structural maturity. We have recently studied the folding pathway of the maltose-binding protein (MBP), a protein containing a discontinuous two-domain fold, using three-color smFRET [29]. We performed specific three-color labeling as described above and used three-color FRET to monitor the conformation of the N-terminal domain (NTD), the C-terminal domain (CTD), and the interface between them (Figure 4e). We observed the real-time folding kinetics of the slow-folding double-mutant (V8G and Y283D) of MBP (DM-MBP), which folds more than an order of magnitude slower than the wild-type protein. It has been previously shown for wild-type MBP that the NTD is able to fold faster than the CTD [42], and other experiments on DM-MBP revealed a folding hysteresis, which indicated a more complex folding [43]. With our three-color FRET experiments, we aimed at distinguishing the intermediate states and the folding order of the two domains. The three-color smFRET experiments were performed in the presence of the denaturant guanidine hydrochloride (GuHCl), allowing us to monitor the conformational changes between all three dye pairs as the protein unfolds and refolds (Figure 4f, g). By having all three distances from the same molecule, we can investigate the conformation of the CTD in proteins where the NTD has folded and visa versa. Our results revealed that the NTD and N–C interface of the protein have to fold first before the folded conformation of the CTD can be stabilized. We could also show that the so-called "intermediate state" is actually due to fluctuations between unfolded and compact conformations on the millisecond timescale. We further studied the MBP system in the presence of the bacterial chaperonin GroEL/ES and demonstrated that the protein is still dynamic, both when bound and when encapsulated within the chaperonin.

Multicolor smFRET studies to explore gene regulation

Recently, a review on DNA and RNA processes has summarized the important developments on the use of multicolor FRET to study various transcriptional phenomena [44] so we focus in this section here on publications that appeared afterwards. Histones are octameric proteins made up of two dimeric H2A-H2B and one tetrameric $(H3–H4)_2$ subunits. Together with the DNA, they are the basic components of chromatin that pack DNA by wrapping it around the histones and release it during transcription. The dynamic behavior of histone proteins is crucial for gene regulation and has been explored by various dual-color smFRET experiments [45–50]. Lee et al. investigated spontaneous histone exchange events between nucleosomes using 3-color smFRET (Figure 5a, b) [51,52]. In the most recent study, they labeled one batch of histones in the DNA region with Cy3-Cy5 and another batch on the H2A-H2B dimer with Cy5.5, mixed the batches (Figure 5a) and measured the change in fluorescence signal resulting from the replacement of the distal or proximal histones (Figure 5b, right panel). The proximal dimer exchanged nucleosomes would lead to a high FRET signal from Cy5.5, which causes premature photobleaching before being properly captured (Figure 5b, right panel, upper trace). Therefore, they used measurements of the distal H2A-H2B dimer probe to compute the exchange rates. Briefly, they counted the traces where a non-zero Cy5.5 signal was coupled to a lowered Cy5 fluorescence, indicating exchanged nucleosomes. Their study revealed that the H2A-H2B subunits undergo assembly-disassembly on a timescale of a few tens of seconds, which is accelerated at higher salt concentrations. This supported the hypothesized disassembly mechanism of the nucleosome as being spontaneous, transient, and partial. They also showed that the histone exchange reactions are faster in the presence of the histone chaperone, nucleosome assembly protein 1 (Nap1), and slower in the case of CpG methylation. With their findings, Lee and co-workers shed light on the mechanisms of histone exchange and could directly visualize processes that influenced its kinetics.

The group of TJ Ha has recently performed a multicolor FRET study on the zinc-finger transcription factor (TF) from *Drosophila melanogaster*, GAF, to reveal the details of how eukaryotic TFs search through the tightly packed

genome during gene expression [53]. Their results demonstrated, for the first time, that eukaryotic TFs combine 1D and 3D diffusional motions as a mechanism of action to target DNA and nucleosomes.

Puglisi et al. studied the role of eukaryotic initiation factors (eIFs) in ribosomal subunit formation. eIFs mediate the formation of the ribosomal subunits on messenger RNA (mRNA), which is necessary to start translation. In four-color FRET experiments, Puglisi et al. could directly observe the formation of the functional 80S ribosomal subunit and the involvement of the eIFs in this process [54]. They aimed to identify whether binding of eIF1A and eIF5B would play a critical role in the formation of the stable ribosomal subunit interactions. In their single-molecule FRET assays, they tethered mRNA strands to zero-mode waveguide (ZMW) surfaces, labeled the ribosomal subunits 40S and 60S, and the initiation factors eIF1A and eIF5B each with different colors of fluorescent dyes (Figure 5c). After loading the readily formed mRNA complex onto the ZMWs, they assessed the positioning of the ribosomal subunits (40S or 60S) and the eFIs (eIF1A or eIF5B) on the RNA strands via the increase in the respective fluorescence signals. In their three-color control experiments, they first visualized the binding of the 40S(Cy3)-eIF1A(Cy5) complex with the associated signal increase and the FRET efficiencies due to their close proximity. The simultaneous presence of both eIF1A and eIF5B on the mRNA–subunit complex is validated by the presence of both FRET signals between eIF1A(Cy3)-eIF5B(Cy3.5) ($R \sim 70$ Å) and 40S(Cy3)-eIF1A(Cy5) ($R \sim 50$ Å). They also performed four-color FRET experiments with the simultaneous addition of all labeled components (subunits 40S and 60S; transcription factors eIF1A and eIF5B), which revealed that the 60S subunit (Cy5.5) binding happens after the dissociation of both eIF1A and eIF5B. Based on their findings from these multicolor FRET experiments, they could kinetically prepare different complexes and used single-particle cryo-electron microscopy (cryo-EM) to visualize how the 80S ribosomal initiation complex forms. In a follow-up study, using a similar multicolor FRET assay, they examined how N^6-methyladenosine (m^6A) modification in the mRNA sequence influences translation initiation (Figure 5e–d) [55]. Their results indicated that a single m^6A modification does not impact overall translation yields nor the kinetics of the initiation complex assembly.

Conclusions and outlook

In this review, we have highlighted the works of many research groups that have enabled multicolor FRET to become a broadly applicable technique to study complex biological processes. These studies include developments of multicolor bioorthogonal labeling strategies and advanced data analysis tools, incorporating AI-driven algorithms to enhance the accuracy and robustness of multicolor FRET applications. We have discussed recent applications of multicolor FRET that have expanded the frontiers of structural biology, offering insights into bimolecular assemblies and their dynamics. In combination with other recent improvements in FRET experiments, such as increasing the observation time via fluorophore exchange [56] or the use of microfluidics [57], multicolor FRET promises to become a powerful tool in the near future.

Funding

D.C.L. gratefully acknowledges funding from the Federal Ministry of Education and Research (BMBF) and the Free State of Bavaria under the Excellence Strategy of the Federal Government and the Länder through the ONE MUNICH Project Munich Multiscale Biofabrication. D.C.L gratefully acknowledges the financial support of the Ludwig-Maximilians-Universität München via the Department of Chemistry, the Center for NanoScience (CeNS), and the LMU innovative program BioImaging Network (BIN).

Declaration of competing interest

The authors declare that they have no known competing financial interests or personal relationships that could have appeared to influence the work reported in this paper.

Data availability

No data was used for the research described in the article.

References

Papers of particular interest, published within the period of review, have been highlighted as:

* of special interest
** of outstanding interest

1. Hellenkamp B, Schmid S, Doroshenko O, Opanasyuk O, Kuhnemuth R, Rezaei Adariani S, Ambrose B, Aznauryan M, Barth A, Birkedal V, *et al.*: **Precision and accuracy of single-molecule FRET measurements-a multi-laboratory benchmark study**. *Nat Methods* 2018, **15**:669–676.

2. Gotz M, Barth A, Bohr SS, Borner R, Chen J, Cordes T, Erie DA, Gebhardt C, Hadzic M, Hamilton GL, *et al.*: **A blind benchmark of analysis tools to infer kinetic rate constants from single-molecule FRET trajectories**. *Nat Commun* 2022, **13**:5402.

3. ** Agam G, Gebhardt C, Popara M, Machtel R, Folz J, Ambrose B, Chamachi N, Chung SY, Craggs TD, de Boer M, *et al.*: **Reliability and accuracy of single-molecule FRET studies for characterization of structural dynamics and distances in proteins**. *Nat Methods* 2023, **20**:523–535.
This international blind study across 19 laboratories established how accurate smFRET experiments can be performed on protein and their conformational dynamics determined. The paper highlights smFRET's analysis details that allow more consistent results and discusses smFRET as a unique tool for the analysis of dynamics in integrative structural biology.

4. Förster T: **Zwischenmolekulare Energiewanderung und Fluoreszenz**. *Ann Phys* 2006, **437**:55–75.

5. Hohng S, Joo C, Ha T: **Single-molecule three-color FRET**. *Biophys J* 2004, **87**:1328–1337.

6. Lee J, Lee S, Ragunathan K, Joo C, Ha T, Hohng S: **Single-molecule four-color FRET**. *Angew Chem Int Ed Engl* 2010, **49**: 9922–9925.

7. Stein IH, Steinhauer C, Tinnefeld P: **Single-molecule four-color FRET visualizes energy-transfer paths on DNA origami**. *J Am Chem Soc* 2011, **133**:4193–4195.

8. Kopperger E, List J, Madhira S, Rothfischer F, Lamb DC, Simmel FC: **A self-assembled nanoscale robotic arm controlled by electric fields**. *Science* 2018, **359**:296–301.

9. Lee NK, Kapanidis AN, Koh HR, Korlann Y, Ho SO, Kim Y, Gassman N, Kim SK, Weiss S: **Three-color alternating-laser excitation of single molecules: monitoring multiple interactions and distances**. *Biophys J* 2007, **92**:303–312.

10. Clamme JP, Deniz AA: **Three-color single-molecule fluorescence resonance energy transfer**. *ChemPhysChem* 2005, **6**: 74–77.

11. Kapanidis AN, Laurence TA, Lee NK, Margeat E, Kong X, Weiss S: **Alternating-laser excitation of single molecules**. *Acc Chem Res* 2005, **38**:523–533.

12. Kapanidis AN, Lee NK, Laurence TA, Doose S, Margeat E, Weiss S: **Fluorescence-aided molecule sorting: analysis of structure and interactions by alternating-laser excitation of single molecules**. *Proc Natl Acad Sci USA* 2004, **101**: 8936–8941.

13. Müller BK, Zaychikov E, Bräuchle C, Lamb DC: **Pulsed interleaved excitation**. *Biophys J* 2005, **89**:3508–3522.

14. Felekyan S, Kalinin S, Valeri A, Seidel C: **Filtered FCS and species cross correlation function**. *Proc SPIE* 2009, **7183**: 71830D.

15. Kalinin S, Felekyan S, Antonik M, Seidel CA: **Probability distribution analysis of single-molecule fluorescence anisotropy and resonance energy transfer**. *J Phys Chem B* 2007, **111**: 10253–10262.

16. * Kudryavtsev V, Sikor M, Kalinin S, Mokranjac D, Seidel CA, Lamb DC: **Combining MFD and PIE for accurate single-pair Forster resonance energy transfer measurements**. *ChemPhysChem* 2012, **13**:1060–1078.
This paper introduces the combination of Multi-parameter Fluorescence Detection with Pulsed Interleaved Excitation (MFD-PIE), which allows for determination of correction factors directly from the data and gives an excellent discussion of how to perform accurate smFRET experiments. This was an essential development for the quantification of multi-color FRET experiments.

17. * Barth A, Voith von Voithenberg L, Lamb DC: **Quantitative single-molecule three-color Forster resonance energy transfer by photon distribution analysis**. *J Phys Chem B* 2019, **123**: 6901–6916.
This works describes the development of the three-color photon distribution analysis, which is a powerful tool for quantifying three-color FRET experiments and thereby extracting coordinated motions within biomolecules.

18. Antonik M, Felekyan S, Gaiduk A, Seidel CA: **Separating structural heterogeneities from stochastic variations in fluorescence resonance energy transfer distributions via photon distribution analysis**. *J Phys Chem B* 2006, **110**:6970–6978.

19. Schrimpf W, Barth A, Hendrix J, Lamb DC: **PAM: a framework for integrated analysis of imaging, single-molecule, and ensemble fluorescence data**. *Biophys J* 2018, **114**:1518–1528.

20. Ha T, Fei J, Schmid S, Lee NK, Gonzalez RL, Paul S, Yeou S: **Fluorescence resonance energy transfer at the single-molecule level**. *Nature Rev Methods Prim* 2024, **4**.

21. Ge L, Liu F, Luo J: **Highly-efficient quantitative fluorescence resonance energy transfer measurements based on deep learning**. *J Innovat Optical Health Sci* 2020, **13**, 2050021.

22. Li J, Zhang L, Johnson-Buck A, Walter NG: **Automatic classification and segmentation of single-molecule fluorescence time traces with deep learning**. *Nat Commun* 2020, **11**:5833.

23. Thomsen J, Sletfjerding MB, Jensen SB, Stella S, Paul B, Malle MG, Montoya G, Petersen TC, Hatzakis NS: **DeepFRET, a software for rapid and automated single-molecule FRET data classification using deep learning**. *eLife* 2020, **9**.

24. ** Wanninger S, Asadiatouei P, Bohlen J, Salem CB, Tinnefeld P, Ploetz E, Lamb DC: **Deep-LASI: deep-learning assisted, single-molecule imaging analysis of multi-color DNA origami structures**. *Nat Commun* 2023, **14**:6564.
This study presents the Deep-Learning Assisted Single-molecule Imaging (Deep-LASI) analysis software suite to analyze multicolor smFRET data acquired from surface-based experiments. It significantly improves the speed and accuracy of smFRET trace classification and dynamic analyses in comparison to manual methods and conventional Hidden Markov Modeling.

25. Asadiatouei P, Salem CB, Wanninger S, Ploetz E, Lamb DC: **Deep-LASI, single-molecule data analysis software**. *Biophys J* 2024, **123**:2682–2695.

26. ** Voith von Voithenberg L, Barth A, Trauschke V, Demarco B, Tyagi S, Koehler C, Lemke EA, Lamb DC: **Comparative analysis of the coordinated motion of Hsp70s from different organelles observed by single-molecule three-color FRET**. *Proc Natl Acad Sci U S A* 2021:118.
This study showcases the application of the newly developed three-color PDA for investigating coordinated motion and conformational changes in proteins using heat shock protein 70s from different species and organelles.

27. Yoo J, Louis JM, Gopich IV, Chung HS: **Three-color single-molecule FRET and fluorescence lifetime analysis of fast protein folding**. *J Phys Chem B* 2018, **122**:11702–11720.

28. Lee TC, Moran CR, Cistrone PA, Dawson PE, Deniz AA: **Site-specific three-color labeling of alpha-synuclein via conjugation to uniquely reactive cysteines during assembly by native chemical ligation**. *Cell Chem Biol* 2018, **25**:797–801 e794.

29. ** Agam G, Barth A, Lamb DC: **Folding pathway of a discontinuous two-domain protein**. *Nat Commun* 2024, **15**: 690.
This work exemplifies how multicolor FRET can be used to determine the order of domain folding in the two-domain, slow-folding double-mutant of the Maltose Binding Protein.

30. Jager M, Nir E, Weiss S: **Site-specific labeling of proteins for single-molecule FRET by combining chemical and enzymatic modification**. *Protein Sci* 2006, **15**:640–646.

31. ** Bonhomme L, Bilgen E, Clerté C, Pin J-P, Rondard P, Margeat E, Lamb DC, Quast RB: **Triple labeling resolves a GPCR intermediate state by 3-color single molecule FRET**. *bioRxiv* 2024, https://doi.org/10.1101/2024.10.31.621373: 2024.2010.2031.621373.
This recent work describes a new specific, bioorthogonal labeling approach to overcome labeling limitations in three-color FRET experiments. The designed triple-labeling strategy is applied to a G protein-coupled receptor, which revealed a previously unknown intermediate state upon antagonist binding.

32. Schmid S, Gotz M, Hugel T: **Effects of inhibitors on Hsp90's conformational dynamics, cochaperone and client interactions**. *ChemPhysChem* 2018, **19**:1716–1721.

33. Wolf S, Sohmen B, Hellenkamp B, Thurn J, Stock G, Hugel T: **Hierarchical dynamics in allostery following ATP hydrolysis monitored by single molecule FRET measurements and MD simulations**. *Chem Sci* 2021, **12**:3350–3359.

34. Gotz M, Wortmann P, Schmid S, Hugel T: **Using three-color single-molecule FRET to study the correlation of protein interactions**. *J Vis Exp* 2018, https://doi.org/10.3791/56896.

35. Ratzke C, Hellenkamp B, Hugel T: **Four-colour FRET reveals directionality in the Hsp90 multicomponent machinery**. *Nat Commun* 2014, **5**:4192.

36. Gotz M, Wortmann P, Schmid S, Hugel T: **A multicolor single-molecule FRET approach to study protein dynamics and interactions simultaneously**. *Methods Enzymol* 2016, **581**: 487–516.

37. Sohmen B, Beck C, Frank V, Seydel T, Hoffmann I, Hermann B, Nuesch M, Grimaldo M, Schreiber F, Wolf S, *et al.*: **The onset of molecule-spanning dynamics in heat shock protein Hsp90**. *Adv Sci (Weinh)* 2023, **10**, e2304262.

38. Marcinowski M, Holler M, Feige MJ, Baerend D, Lamb DC, Buchner J: **Substrate discrimination of the chaperone BiP by autonomous and cochaperone-regulated conformational transitions**. *Nat Struct Mol Biol* 2011, **18**:150–158.

39. Sikor M, Mapa K, von Voithenberg LV, Mokranjac D, Lamb DC: **Real-time observation of the conformational dynamics of mitochondrial Hsp70 by spFRET**. *EMBO J* 2013, **32**: 1639–1649.

40. Andryushchenko VA, Chekmarev SF: **Modeling of multicolor single-molecule forster resonance energy-transfer experiments on protein folding**. *J Phys Chem B* 2018, **122**: 10678–10685.

41. ** Yoo J, Kim JY, Louis JM, Gopich IV, Chung HS: **Fast three-color single-molecule FRET using statistical inference**. *Nat Commun* 2020, **11**:3336.
This study presents a three-color FRET approach for investigating folding transitions during the folding of a small peptide. It uses single continuous-wave laser excitation to overcome photophysical issues like rapid acceptor photobleaching.

42. Walters BT, Mayne L, Hinshaw JR, Sosnick TR, Englander SW: **Folding of a large protein at high structural resolution**. *Proc Natl Acad Sci U S A* 2013, **110**:18898–18903.

43. Chakraborty K, Chatila M, Sinha J, Shi Q, Poschner BC, Sikor M, Jiang G, Lamb DC, Hartl FU, Hayer-Hartl M: **Chaperonin-catalyzed rescue of kinetically trapped states in protein folding**. *Cell* 2010, **142**:112–122.

44. Feng XA, Poyton MF, Ha T: **Multicolor single-molecule FRET for DNA and RNA processes**. *Curr Opin Struct Biol* 2021, **70**: 26–33.

45. Fierz B: **Dynamic chromatin regulation from a single molecule perspective**. *ACS Chem Biol* 2016, **11**:609–620.

46. Kilic S, Felekyan S, Doroshenko O, Boichenko I, Dimura M, Vardanyan H, Bryan LC, Arya G, Seidel CAM, Fierz B: **Single-molecule FRET reveals multiscale chromatin dynamics modulated by HP1alpha**. *Nat Commun* 2018, **9**:235.

47. Lehmann K, Felekyan S, Kuhnemuth R, Dimura M, Toth K, Seidel CAM, Langowski J: **Dynamics of the nucleosomal histone H3 N-terminal tail revealed by high precision single-molecule FRET**. *Nucleic Acids Res* 2020, **48**:1551–1571.

48. Poyton MF, Feng XA, Ranjan A, Lei Q, Wang F, Zarb JS, Louder RK, Park G, Jo MH, Ye J, *et al.*: **Coordinated DNA and histone dynamics drive accurate histone H2A.Z exchange**. *Sci Adv* 2022, **8**, eabj5509.

49. Huynh MT, Sengupta B, Krajewski WA, Lee TH: **Effects of histone H2B ubiquitylations and H3K79me(3) on transcription elongation**. *ACS Chem Biol* 2023, **18**:537–548.

50. ** Das SK, Huynh MT, Gao J, Sengupta B, Yadav SP, Lee TH: **Methods to investigate nucleosome structure and dynamics with single-molecule FRET**. *Methods* 2023, **215**: 17–27.
This study highlights the use of three-color smFRET to investigate the kinetics of histone exchange between nucleosomes and elucidate the influence of salt concentrations, histone modifications, and chaperones on the dynamics of the process.

51. Lee J, Lee TH: **Single-molecule investigations on histone H2A-H2B dynamics in the nucleosome**. *Biochemistry* 2017, **56**: 977–985.

52. Das SK, Huynh MT, Lee TH: **Spontaneous histone exchange between nucleosomes**. *J Biol Chem* 2023, **299**, 105037.

53. Feng XA, Yamadi M, Fu Y, Ness KM, Liu C, Ahmed I, Bowman GD, Johnson ME, Ha T, Wu C: **GAGA zinc finger transcription factor searches chromatin by 1D-3D facilitated diffusion**. *bioRxiv* 2024, https://doi.org/10.1101/2023.07.14.549009.

54. ** Lapointe CP, Grosely R, Sokabe M, Alvarado C, Wang J, Montabana E, Villa N, Shin BS, Dever TE, Fraser CS, *et al.*: **eIF5B and eIF1A reorient initiator tRNA to allow ribosomal subunit joining**. *Nature* 2022, **607**:185–190.
This study showcases the use of three-color and four-color smFRET experiments to reveal how eIF1A and eIF5B coordinate ribosomal assembly, which is a key step in translation initiation in cells.

55. ** Guca E, Alarcon R, Palo MZ, Santos L, Alonso-Gil S, Davyt M, de Lima LHF, Boissier F, Das S, Zagrovic B, *et al.*: **N6-methyladenosine in 5' UTR does not promote translation initiation**. *Mol Cell* 2024, **84**:584–595.e586.
This study showcases the use of three-color smFRET experiments to reveal how mRNA modifications can influence the tranlation efficiency and the ribosomal initiation complex formation knitetics.

56. * Vermeer B, Schmid S: **Can DyeCycling break the photobleaching limit in single-molecule FRET?** *Nano Res* 2022, **15**: 9818–9830.
This paper introduces the concept of "DyeCycling" to overcoming the photobleaching limitations of single molecule FRET measurements during an experiment, allow observation times of hours on a single molecule.

57. * Benke S, Holla A, Wunderlich B, Soranno A, Nettels D, Schuler B: **Combining rapid microfluidic mixing and three-color single-molecule FRET for probing the kinetics of protein conformational changes**. *J Phys Chem B* 2021, **125**:6617–6628.
A rapid microfluidic mixing method is described in this paper that allows protein conformational changes to be investigated over a wide range of time scales, from milliseconds to minutes. It was applied to observe monomer-to-protomer conversion of cytolysin A using three-color FRET experiments. A previously undetected intermediate state was revealed.